Electron-spin resonance studies of the titanium cation (Ti^+,$3d^3$,^4F) in rare gas matrices at 4 K: A crystal field interpretation

Lon B. Knight, Jr., Keith A. Keller, and Robert M. Babb
Department of Chemistry, Furman University, Greenville, South Carolina 29613

Michael D. Morse
Department of Chemistry, University of Utah, Salt Lake City, Utah 84112

(Received 3 May 1996; accepted 25 June 1996)

Electron-spin resonance studies of laser-ablated titanium metal isolated in neon and argon display an intense feature which exhibits a symmetric, narrow line and a large matrix-dependent g shift. On the basis of a number of experiments, this is assigned to a matrix isolated $3d^3,^4F$ Ti^+ ion in an octahedral matrix environment. Although the ground state of the gas-phase Ti^+ ion is $3d^2 4s^1,^4F$, the assignment to the $3d^3,^4F$ state is supported by the small hyperfine structure which is observed. The neon magnetic parameters are: $g=1.934(1)$ and $A(^{47}Ti)=64(1)$ MHz; for argon, $g=1.972(1)$ and $A=56(1)$ MHz. This unusual stabilization of an excited atomic state by a rare gas matrix is consistent with *ab initio* studies, and has been previously found for atomic nickel. A crystal-field study of the expected behavior of a $d^3,^4F$ ion isolated in a tetrahedral, octahedral, or cuboctahedral environment supports the assignment to an octahedral $Ti^+(Rg)_6$ species, and using the atomic spin–orbit parameter, ζ permits accurate values of Dq to be derived from the measured g values. Finally, it is also noted that for small values of $Dq/(Dq+\zeta)$, or for a $d^3,^4F$ ion in a tetrahedral environment, an as yet unobserved, unequal Zeeman splitting of the fourfold degeneracy occurs, causing a departure of the Zeeman energies from the standard formula of $E^{\text{Zeeman}}=\beta_e H_0 g M$, with $M=\pm 3/2, \pm 1/2$. For these situations it becomes necessary to define two values of g, corresponding to the more strongly ($g_{3/2}$) and less strongly ($g_{1/2}$) affected Zeeman levels, respectively. © *1996 American Institute of Physics.* [S0021-9606(96)00937-3]

I. INTRODUCTION

In this paper ESR (electron-spin resonance) spectra are presented for Ti^+ atomic ions isolated in neon and argon matrices. These spectra are unusual because the gaseous Ti^+ ion has an orbitally degenerate $3d^2 4s^1,^4F$ ground state and an orbitally degenerate $3d^3,^4F$ first excited state lying 908 cm^{-1} above the ground state.[1] In fact, all of the known electronic states of gaseous Ti^+ lying below 21 000 cm^{-1} possess orbital degeneracy.[1] ESR detection of an orbitally degenerate metal ion isolated in a rare gas matrix has not been previously reported.[2] Given the role of titanium and its compounds in numerous catalytic and chemisorption applications, it is important to understand various types of titanium bonding and electronic structures. These new ESR results provide an unusual opportunity to probe the interaction of a metal ion with rare gas atoms.

The ESR matrix observations presented and analyzed in this paper are assigned to Ti^+ radicals in an octahedral interstitial site in the rare gas fcc lattice. This site is of nearly optimal size for the Ti^+ ion, based on theoretical calculations of the Ti^+–Ne and Ti^+–Ar interactions,[3] and an octahedral site is also suggested by the unusual stability of the cobalt ion–rare gas complex, $CoAr_6^+$, in supersonic expansions of Co^+ in argon.[4] The theoretical calculations of Ti^+–Ne and Ti^+–Ar interactions also strongly support the assignment of the $3d^3,^4F$ state as the ground state of matrix isolated Ti^+,[3] in agreement with the small hyperfine splitting found in the present study for the magnetic $^{47}Ti(I=5/2$; 7.3% nat'l abund.) and $^{49}Ti(I=7/2$; 5.5% nat'l abund.) nuclei. The small hyperfine interaction is attributed to the absence of direct $4s$ admixture in the $3d^3$ configuration. Although unusual, this reversal in the ordering of the $3d^2 4s^1,^4F$ and $3d^3,^4F$ states of Ti^+ in moving from the gas phase to the neon or argon matrix is not unprecedented. Previous studies of matrix isolated nickel atoms using optical spectroscopy have indicated a shift from the $3d^8 4s^2,^3F_4$ gas phase ground state to a $3d^9 4s^1,^3D_3$ ground state in Ar, Kr, and Xe matrices.[5] In the case of nickel the gas phase separation between these two states is only 205 cm^{-1}; for Ti^+ the separation between the $3d^2 4s^1,^4F_{3/2}$ and $3d^3,^4F_{3/2}$ states is 908 cm^{-1}.

The quenching of the orbital angular momentum of the $3d^3,^4F$ state of Ti^+ in the octahedral interstitial site may be understood by considering the dipole and higher multipole moments induced in the surrounding rare gas atoms as providing a weak ligand field, which splits the ^4F term into $^4A_{2g}$, $^4T_{1g}$, and $^4T_{2g}$ terms, with the $^4A_{2g}$ term lying lowest in energy. The relatively small splitting between these terms accentuates the spin–orbit interactions and perturbs the $^4A_{2g}$ ground state, creating an admixture of this state with the higher lying $^4T_{1g}$ and $^4T_{2g}$ terms. This results in a significant reduction of the observed g value from the free-electron value of 2.0023. Moreover, the different crystal field splittings in argon versus neon causes this shift in the g value from g_e to be quite different in the different rare gas matrices. Included in the present experimental study is a theoretical treatment of the ligand field and spin–orbit interactions. This permits the g value to be predicted as a function of the ligand field strength, Dq, and the spin–orbit parameter, ζ.

This theoretical treatment also supports the hypothesis that the Ti^+ ion is trapped in an octahedral matrix site.

The large observed change in the g value going from neon [1.934(1)] to argon [1.972(1)] would be unprecedented if the ESR spectrum of a titanium containing molecular species was being observed.[6] The neon–argon g shift is consistent with the crystal field model developed in this study to help account for these experimental findings because the crystal field splitting expected for the $TiNe_6^+$ species is less than that expected for $TiAr_6^+$. This results in less quenching of the orbital angular momentum and a greater departure from g_e in the case of neon as compared to argon. A similar degree of sensitivity of the g value to the rare gas matrix has also been observed for aluminum and gallium atoms, which have orbitally degenerate $^2P^0_{r_2}$ gas phase ground states.[7] Trapping sites which provide a nearly axially symmetric environment produce varying degrees of orbital quenching, the extent of which depends upon the matrix host employed. Atomic aluminum, for example, exhibits a neon matrix $g_\perp$ value of 1.925 compared to 1.952 for an argon matrix. This environmentally sensitive atomic g tensor behavior stands in sharp contrast to all ESR observations of rare gas isolated molecular radicals. In molecular cases the g values are virtually the same regardless of the rare gas host, both for neutral and charged molecules.

Experimental results confirm that the titanium species observed in the present experiment is charged and contains only one titanium atom. Likely impurities in such experiments involving the pulsed laser vaporization of titanium metal are the TiO, TiO^+ and TiO_2 molecules. None of these, however, have the appropriate electronic ground state to account for the observed ESR spectrum. The electronic ground states of TiO[8] and TiO^+[9] are known to be $X\ ^3\Delta$ and $X\ ^2\Delta$, respectively, while TiO_2 is expected to have a singlet ground state.

The rare gas matrix isolation technique for ESR investigations has been described in previous accounts.[6,10–13] The number of titanium containing radicals studied by this method is quite small. Systems reported to date include TiF_2 and TiF_3,[6] and the intermetallic molecules TiCo,[14] TiV,[15] and TiNb.[16] Argon matrix isolation Fourier transform infrared studies have identified several new titanium molecules, including TiN_2, O_2TiN_2, $O_2Ti(N_2)_2$ and OTiCO.[17] These studies also involved the laser ablation of titanium metal as the source of Ti atoms.

II. EXPERIMENT

The ESR matrix isolation apparatus employed in our laboratory at Furman University for trapping the products of pulsed laser ablation has been described previously.[12,18] A special feature of this system shown in Fig. 1 is the ability to electrically deflect charged species, thus preventing them from being trapped in the matrix. This capability was particularly useful in the present experiments by supporting the assignment of the ESR spectrum to a matrix isolated ion radical.

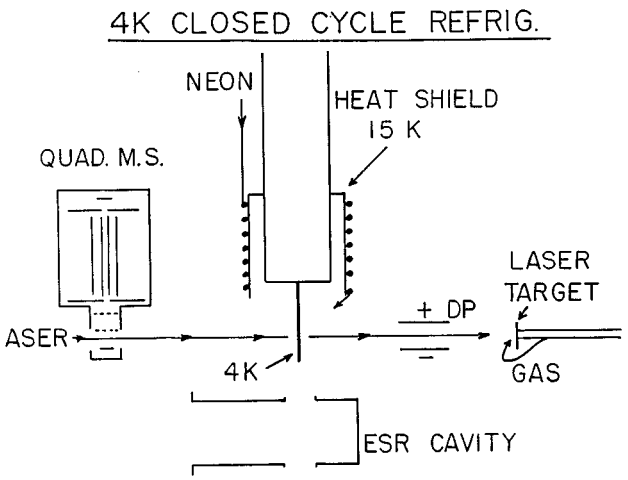

FIG. 1. The matrix isolation ESR apparatus used in these experiments to trap Ti^+ in neon and argon matrices is shown. The laser target was a titanium plate. The electric deflection plates used to discriminate between the trapping of neutral and charged species are labeled ''DP.''

The observed ESR absorptions assigned to Ti^+ in neon and argon matrices at 4 K were produced by two independent generation methods. The pulsed laser vaporization (PLV) production of matrix isolated Ti^+ was achieved by focusing the frequency doubled output (532 nm, ≈20 mJ/pulse) of a Nd:YAG laser operating at 10 Hz onto a titanium metal target. For those experiments not involving electrical deflection, the Ti target was located 5 cm from the matrix deposition surface. A closed cycle 4 K refrigerator (APD HS-4) was employed to cool the flat copper matrix deposition surface. In the experimental arrangement where deposition results obtained with and without electrical deflection were directly compared, the titanium target was located 15 cm from the matrix deposition surface. The greater distance in these experiments was necessitated by the presence of the electrical deflection plates.

A continuous rare gas flow of 5 std. $cm^3\,min^{-1}$ was used, with typical depositions conducted for 40 min. The laser beam, focused to a spot size of approximately 0.3 mm, was slowly moved across the titanium surface by means of a focusing lens which was external to the vacuum chamber of the cryostat system. Prior to deposition, the background pressure was approximately 5×10^{-8} Torr. Standard helium mass spectrometric leak testing was conducted prior to each deposition experiment. Matheson research grade rare gases were passed through liquid nitrogen cooled traps and cooled molecular sieve traps immediately prior to entering the deposition chamber. The titanium metal (3-mm-thick plate, metallic purity 99.999%) was obtained from Alfa.

The positively charged ions produced under these PLV conditions were also monitored with a quadrupole mass spectrometer (QMS). A transverse ion collection geometry was employed, with the sample beam entering the collection optics at 90° to the center axis of the quadrupole rods. The QMS detection system, which included a LeCroy 9400A storage scope, was gated to the firing of the PLV with delay

times controlled by a Stanford model DG 535 pulse generator. The QMS mass sweep was slowly advanced over the range of 1–250 amu with sufficiently long dwell times to obtain signal averaged measurements. The electron emission filament of the QMS was not operated during these ion monitoring experiments. Intense Ti^+ signals along with weak hydrocarbon background ions (i.e., $C_3H_5^+$) and barely detectable amounts of TiO^+ were observed. Over short time periods (10–20 s) the oxide ion signal virtually disappeared unless the laser beam was moved to a ''fresh'' area of the titanium metal surface. The experimental information obtained from these direct QMS measurements was useful in optimizing the Ti^+ generation conditions employed in the matrix trapping ESR experiments—such as laser pulse energies, degree of focusing, and rate of laser movement across the Ti surface.

The second generation method employed for isolating Ti^+ radicals in neon and argon matrices involved the thermal vaporization of a titanium rod. A 5 cm rod with a thin section machined in the center was mounted across two water cooled copper electrodes and was positioned approximately 10 cm from the matrix deposition surface. Using an Ultimax infrared pyrometer to measure the temperature, the sample was resistively heated to just below the melting point of titanium. Over a 30 min deposition period, a thin metallic film of titanium was observed to form on a view window located just beside the matrix target. ESR spectra recorded for matrices formed under these thermal vaporization conditions did not exhibit the features assigned to Ti^+ and did not show evidence of any other titanium-containing radicals. Background absorptions resulting from isolated CH_3 were observed, as is typically the case under such high energy trapping conditions. The ratio of rare gas atoms to Ti^+ is approximately 30 000 to 1 based upon the amount of sublimed titanium, various assumptions concerning the amount of rare gas that condenses, and the extent to which neutral titanium atoms are ionized.

The x irradiation of these neon and argon matrices containing thermally generated Ti atoms produced exactly the same ESR absorptions assigned to Ti^+ in the PLV depositions. This method has been proven to be an effective means of generating radical ions of matrix isolated atoms and small molecules.[19–22] Our experimental arrangement for x-irradiating matrix samples after deposition has been described in the recent ESR reports on CH_3OH^+, CH_4^+, H_2O^+, Mg^+, and Sc_2^+.[19,20,22] The same equipment and procedures were employed in these titanium atom matrix experiments, with x-ray energies in the 50–60 keV range and irradiation times of 20 min.

III. ESR RESULTS

The observed neon and argon ESR spectra obtained for the matrix samples prepared by pulsed laser vaporization of titanium metal are shown in Fig. 2. Nearly identical spectra were also observed for x-irradiated matrices which contained titanium atoms deposited by thermal evaporation of the metal. The magnetic centers of the background methyl radi-

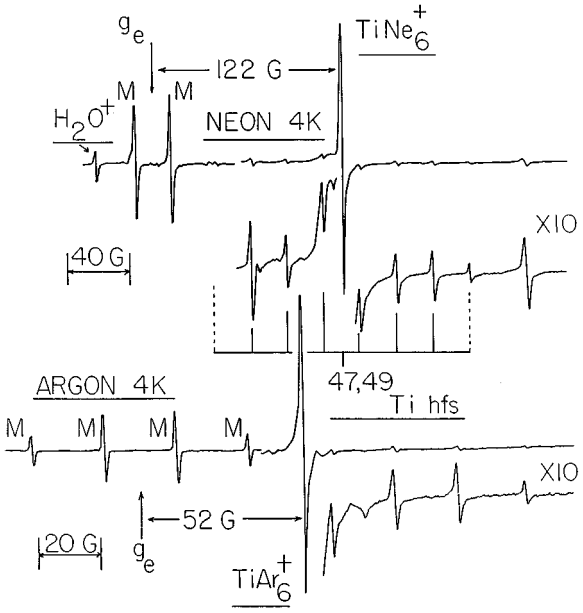

FIG. 2. The ESR spectra assigned to Ti^+ isolated in neon (top spectrum) and argon (bottom spectrum) matrices at 4 K are shown. Methyl (CH_3) radical signals are designated ''*M*'' and ''g_e'' represents the magnetic field position corresponding to $g=2.0023$. Absorption features of other background impurity radicals, including H_2O^+ and H atoms are labeled accordingly. The intense symmetric line 122 G above g_e in neon and 52 G above g_e in argon is assigned to Ti^+ ($I=0$) trapped in an octahedral matrix site. The weaker sextet and octet nuclear hfs of the $^{47}Ti(I=5/2)$ and $^{49}Ti(I=7/2)$ isotopes are labeled for the neon spectrum for the segment that has been expanded vertically by a factor of 10.

cal quartet absorptions (M) have been carefully aligned for these neon and argon spectra in order to illustrate the pronounced g shift of the high field, symmetric line assigned to $Ti^+(Rg)_6$. The CH_3 radical has essentially the same g value of 2.002 in both rare gases.[6,23] Note that the $Ti^+(Rg)_6$ absorption is highly symmetric and is shifted upfield from g_e by 122 G in neon and 52 G in argon. Attempts to observe this feature in krypton matrices yielded a broad line approximately 10 G above g_e, but a confident assignment for krypton could not be made since the absorption was considerably less intense and the characteristic hyperfine patterns of the magnetic isotopes of titanium could not be fully analyzed in this more congested spectral region.

The intense and highly symmetric absorption line assigned to matrix isolated Ti^+ cation radicals was accompanied by symmetric satellite features in both neon and argon hosts. As indicated in Fig. 2, these sextet and octet patterns are assigned to the less abundant magnetic isotopes of titanium, namely $^{47}Ti(I=5/2;\ 7.28\%)$ and $^{49}Ti(I=7/2;\ 5.51\%)$. The six inner lines of the octet hyperfine pattern overlap the sextet pattern since the nuclear g factors (μ/I) for these two isotopes are nearly identical, namely, 0.3154 vs 0.3155. Note that the eighth component (the dashed line designation in Fig. 2) of the octet belonging to ^{49}Ti is considerably weaker than the seventh component of ^{49}Ti which is overlapped by the sixth component of the ^{47}Ti sextet hyperfine pattern. Highly expanded spectra were recorded so that accurate integrated intensities of the various lines could be measured and compared to similar measurements for the unsplit Ti^+

central line arising from those titanium isotopes with $I=0$. These integrated intensity measurements were consistent with the ESR assignment to a radical species containing a single titanium atom.

Using our exact diagonalization programs and standard line fitting procedures,[24] calculated line positions showed agreement with the observed positions within the experimental uncertainty of ± 0.3 G in both rare gases. For neon the magnetic parameters are: $g=1.934(1)$ and $A(^{47}\mathrm{Ti})=64(1)$ MHz. The argon results are: $g=1.972(1)$ and $A(^{47}\mathrm{Ti})=56(1)$ MHz. For a given matrix, the same g value results were obtained from independent analyses of the strong unsplit central line and the hyperfine patterns associated with ^{47}Ti and ^{49}Ti.

Supporting evidence that the observed ESR features assigned to matrix isolated Ti^+ were in fact associated with a charged radical was obtained from visible light photolysis experiments. Visible light irradiation of the matrix sample over a 20 min period completely eliminated all of the ESR absorptions assigned to Ti^+. This is a well-established diagnostic test for the presence of isolated ions in rare gas matrices.[12,25] Absorptions associated with neutral radicals such as methyl and hydrogen atoms are not affected by such photolysis. Visible light contains sufficient energy to photoionize the anion species in the matrix. The liberated electrons can travel long distances throughout the rare gas lattice and neutralize the cations, thereby eliminating their ESR absorptions. Other evidence supporting the ESR assignment to a charged radical was the pulsed laser deposition of titanium when approximately 400 V was applied to the deflection plates (see Fig. 1). None of the ESR features assigned to Ti^+ were observed under such conditions. The trapping of neutral radicals should not be affected by the presence of such fields. Based on previous studies of rare gas matrix isolated charged species, the most likely counteranion in these titanium experiments is OH^- which can be generated in abundance from a background amount of H_2O.[10–13,25] While OH^- cannot be detected by ESR, several other anions have been observed, including F_2^-, CO_2^-, and $F_2\,CO^-$.[12,13]

Several experiments were conducted to determine whether the presence of oxygen during deposition had any influence on the ESR features assigned to Ti^+ since titanium oxides would be expected to be the most likely impurities. The addition of O_2(g), either premixed with the matrix gas or passed directly over the titanium surface undergoing laser vaporization, caused a more than tenfold decrease in the Ti^+ ESR signals. The position of the gas inlet tube relative to the titanium target is shown in Fig. 1. Also pulsed laser vaporization of TiO_2 or a Ti–TiO_2 mixture produced extremely weak Ti^+ signals. Depositions conducted in the presence of N_2, CO_2, and H_2O also produced no enhancement in the Ti^+ ESR absorptions.

In addition to these tests which imply that the carrier of the spectrum is a matrix isolated Ti^+ ion, the observed ESR absorptions are unusually narrow and symmetric. The peak-to-peak linewidth is approximately 1.8 G in neon and only slightly larger in argon. Except for a reduction in intensity, no significant spectral changes were caused by warming the neon matrix to 10 K and argon to 32 K. The unusually narrow and symmetrical line shape suggests that the Ti^+ ion is located in an environment which produces a D tensor (zero field splitting) of zero, so that the three allowed fine structure transitions ($\Delta M_S=1$) for this quartet spin state occur at precisely the same magnetic field position, which is determined solely by the g value. A D tensor of zero is required on group theoretical grounds only for sites having tetrahedral, octahedral, or icosahedral local symmetry, and for this reason we limit our consideration of the various possible Ti^+ environments to these symmetries.

IV. CRYSTAL FIELD INTERPRETATION

A. Possible high-symmetry sites

With the exception of helium, all of the rare gases condense to form a fcc lattice, with 4 K lattice parameters, a, of 4.462, 5.312, 5.644, and 6.131 Å for Ne, Ar, Kr, and Xe, respectively.[26,27] Assuming that the rare gas lattice retains its structural integrity when Ti^+ is deposited into it, only three high-symmetry environments are possible for the Ti^+ ion: (i) a cuboctahedral substitutional site with 12 nearest neighbors located at a distance of $a/\sqrt{2}$, having a local symmetry of O_h, (ii) an octahedral interstitial site with 6 nearest neighbors located at a distance of $a/2$, having a local symmetry of O_h, and (iii) a tetrahedral interstitial site with 4 nearest neighbors located at a distance of $a\sqrt{3/4}$, having a local symmetry of T_d. For neon (argon) the distances between the Ti^+ ion and the neighboring rare gas atoms work out to 3.155 (3.756), 2.231 (2.656), and 1.932 Å (2.300 Å), for sites (i), (ii), and (iii), respectively. These compare to equilibrium bond lengths obtained in a sophisticated *ab initio* calculation for the $^4\Phi$ ground states of $TiNe^+$ and $TiAr^+$ of 2.43 and 2.65 Å, respectively.[3] The close correspondence between the equilibrium bond lengths in the $TiNe^+$ and $TiAr^+$ cations and the Ti^+–rare gas distances for site (ii) strongly suggests that the high symmetry site occupied by the Ti^+ ion in the matrix is the octahedral interstitial site. In all likelihood there will also be some local distortion of the lattice around the Ti^+ ion, even when it is placed in the octahedral interstitial site, but the near correspondence in distances for this site and the $TiNe^+$ and $TiAr^+$ molecules suggests that only a slight lattice distortion will be required. The crystal field calculations presented below also provide strong support of an octahedral interstitial site, and argue strongly against the cuboctahedral substitutional or tetrahedral interstitial sites.

The *ab initio* calculations of transition metal ion–rare gas interactions reported by Partridge and Bauschlicher generally demonstrate much stronger bonding for transition metal ions in $3d^{n+1}4s^0$ configurations as compared to $3d^n4s^1$ configurations.[3] In addition, for the cases of V^+, Cr^+, Fe^+, and Co^+ little configurational mixing between the $3d^{n+1}4s^0$ and $3d^n4s^1$ configurations was found, presumably because in these metals these configurations are separated by at least 1870 cm^{-1}. In the case of Ti^+, however, the smaller separation between the $3d^24s^1,{}^4F$ and $3d^3,{}^4F$ asymptotes (908 cm^{-1}) permitted strong mixing of these configurations. In particular, the $^4\Phi$ states corresponding to the

$|3d\delta_{+2}\alpha 3d\pi_{+1}\alpha 4s\sigma\alpha|$ and $|3d\delta_{+2}\alpha 3d\pi_{+1}\alpha 3d\sigma\alpha|$ configurations are strongly mixed, effectively removing electron density from the $4s$ orbital by $s-d$ hybridization. This mechanism pushes electron density off of the z axis, permitting a closer approach of the rare gas atom. It also implies that a second rare gas atom will attach to form a linear triatomic complex, such as Ne–Ti^+–Ne.

When more than two rare gas ligands are involved, the mechanism of $3d-4s$ hybridization becomes ineffective because the electron density pushed off of the z axis prevents close approach of the subsequent ligands.[3] Thus there is a strong preference to remove the relatively diffuse $4s$ electron density by promoting the system to the $3d^3,{}^4F$ state. A qualitative estimate of the differential stabilization for Ti^+ interacting with six argon atoms in its $3d^3$ vs $3d^24s^1$ configurations may be obtained by comparison to *ab initio* results for V^+ interacting with argon. The bond energy calculated for VAr^+ in its $3d^4$, $^5\Sigma^+$ ground state is 0.322 eV, as compared to the most strongly bound state arising from the $3d^34s^1,{}^5F$ configuration, which is bound by 0.089 eV.[3] If one could assume that this binding energy difference of 0.233 eV is repeated for the addition of five more argon ligands, the $3d^4$ configuration of VAr_6^+ would be stabilized by 14 eV relative to the $3d^34s^1$ configuration. Given the near degeneracy of the $3d^3,{}^4F$ and $3d^24s^1,{}^4F$ states in the isolated Ti^+ ion, it seems clear that the $3d^3$ configuration will be greatly favored for the octahedral $TiAr_6^+$ complex. Presumably it is also favored for the $TiNe_6^+$ complex, although to a lesser degree.

Along these lines, the Bowers group has used the technique of gas-phase ion chromatography to investigate species such as $Ti(H_2)_n^+$ and $Ti(CH_4)_n^+$. In both $Ti(H_2)^+$ and $Ti(CH_4)^+$ the weak interaction with the single H_2 or CH_4 ligand is nevertheless sufficient to stabilize the $3d^3$ configuration over the $3d^24s^1$ configuration.[28,29] In related work the Bowers group has observed that coordination of a single H_2 molecule to Fe^+ is sufficient to change the ground state from $3d^64s^1$ to $3d^74s^0$, despite the fact that the $3d^74s^0,{}^4F_{9/2}$ level of Fe^+ lies 1873 cm^{-1} above the $3d^64s^1,{}^6D_{9/2}$ ground level.[30] For Sc^+, on the other hand, coordination of three H_2 molecules is required to change the ground state from $3d^14s^1,{}^3D_1$ to $3d^24s^0,{}^3F_2$.[31] This presumably results from the higher promotion energy in the case of Sc^+, where the $3d^24s^0,{}^3F_2$ level lies 4802 cm^{-1} above the $3d^14s^1,{}^3D_1$ ground level. Finally, Mn^+ remains $3d^54s^1$, even when up to six H_2 molecules are coordinated.[32] In this case the high promotion energy of 14 325 cm^{-1} required to convert Mn^+ from $3d^54s^1,{}^7S_3$ to $3d^64s^0,{}^5D_4$ simply cannot be overcome.

B. Crystal field theory for a $d^3,{}^4F$ ion

A set of 28 basis functions corresponding to the $3d^3,{}^4F$ term may be readily generated by starting with the $M_L=3,M_S=3/2$ function, given by the Slater determinant $|d_{+2}\alpha(1)d_{+1}\alpha(2)d_0\alpha(3)|$ and applying the spin and orbital angular momentum lowering operators. In this case it is possible to separate the spin and spatial portions of the wave function, because the $(M_L=3,M_S=3/2)$ basis function factors into a spatial function, $|d_{+2}(1)d_{+1}(2)d_0(3)|$, times a spin function, $\alpha(1)\ \alpha(2)\ \alpha(3)$. Thus, in this case, the overall wave function is the product of a spatial function which is antisymmetric with respect to the interchange of any two electrons times a spin function which is symmetric with respect to the interchange of any two electrons. Applying the lowering operators then leads to a set of four symmetric spin functions $(S=3/2,M_S)$ and a set of seven antisymmetric spatial functions $(L=3,M_L)$, listed in Table I. The 28 possible basis functions are the products of these two sets. Because L and S are fixed, the basis functions may be labeled simply by (M_L,M_S).

TABLE I. Basis wave functions for the $3d^3$, ^4F state of Ti^+.

Spin functions for $S=3/2$ (S,M_S)		Spatial wave functions for $L=3$ (L,M_L)[a]	
(3/2,3/2)	$\alpha(1)\alpha(2)\alpha(3)$	(3,3)	$\lvert d_{+2}d_{+1}d_0\rvert$
(3/2,1/2)	$[\alpha(1)\alpha(2)\beta(3)+\alpha(1)\beta(2)\alpha(3)+\beta(1)\alpha(2)\alpha(3)]/\sqrt{3}$	(3,2)	$\lvert d_{+2}d_{+1}d_{-1}\rvert$
(3/2,−1/2)	$[\beta(1)\beta(2)\alpha(3)+\beta(1)\alpha(2)\beta(3)+\alpha(1)\beta(2)\beta(3)]/\sqrt{3}$	(3,1)	$\sqrt{3/5}\lvert d_{+2}d_0d_{-1}\rvert + \sqrt{2/5}\lvert d_{+2}d_{+1}d_{-2}\rvert$
(3/2,−3/2)	$\beta(1)\beta(2)\beta(3)$	(3,0)	$1/\sqrt{5}\lvert d_{+1}d_0d_{-1}\rvert + 2/\sqrt{5}\lvert d_{+2}d_0d_{-2}\rvert$
		(3,−1)	$\sqrt{3/5}\lvert d_{+1}d_0d_{-2}\rvert + \sqrt{2/5}\lvert d_{+2}d_{-1}d_{-2}\rvert$
		(3,−2)	$\lvert d_{+1}d_{-1}d_{-2}\rvert$
		(3,−3)	$\lvert d_0d_{-1}d_{-2}\rvert$

[a]In all cases, the spatial wave function is written as a Slater determinant to ensure that it is antisymmetric under the exchange of any two electrons.

Two operators contribute to the Hamiltonian of the system in the absence of an external field: (i) a crystal field Hamiltonian, $\hat{H}^{CF}$ and (ii) the spin–orbit Hamiltonian, $\hat{H}^{SO}$. For the O_h or T_d symmetries of sites (i), (ii), or (iii), the crystal field Hamiltonian has nonzero matrix elements, $\langle M_L,M_S|\hat{H}^{CF}|M_L',M_S'\rangle$, only for $M_S=M_S'$, $M_L=M_L'$, $M_L'\pm 4$. The spin–orbit Hamiltonian has nonzero matrix elements, $\langle M_L,M_S|\hat{H}^{SO}|M_L',M_S'\rangle$, only for $M_S=M_S'$, $M_L=M_L'$; $M_S=M_S'+1, M_L=M_L'-1$; and $M_S=M_S'-1, M_L=M_L'+1$. These patterns of nonzero Hamiltonian matrix elements allow the set of 28 basis functions to be broken up into noninteracting blocks consisting of the (M_L,M_S) basis functions as follows:

$$\text{block 1: } \{(3,3/2),(2,-3/2),(1,-1/2),(0,1/2),(-1,3/2),(-2,-3/2),(-3,-1/2)\},$$

$$\text{block 2: } \{(3,1/2),(2,3/2),(1,-3/2),(0,-1/2),(-1,1/2),(-2,3/2),(-3,-3/2)\},$$

TABLE II. Hamiltonian matrices including crystal field and spin–orbit interactions.

block 1: $(3,\frac{3}{2})$	$(2,-\frac{3}{2})$	$(1,-\frac{1}{2})$	$(0,\frac{1}{2})$	$(-1,\frac{3}{2})$	$(-2,-\frac{3}{2})$	$(-3,-\frac{1}{2})$
$3Dq+3\zeta/2$	0	0	0	$\sqrt{15}Dq$	0	0
0	$-7Dq-\zeta$	$\sqrt{5}\zeta/\sqrt{6}$	0	0	$5Dq$	0
0	$\sqrt{5}\zeta/\sqrt{6}$	$Dq-\zeta/6$	$2\zeta/\sqrt{3}$	0	0	$\sqrt{15}Dq$
0	0	$2\zeta/\sqrt{3}$	$6Dq$	ζ	0	0
$\sqrt{15}Dq$	0	0	ζ	$Dq-\zeta/2$	0	0
0	$5Dq$	0	0	0	$-7Dq+\zeta$	$\zeta/\sqrt{2}$
0	0	$\sqrt{15}Dq$	0	0	$\zeta/\sqrt{2}$	$3Dq+\zeta/2$

block 3: $(3,-\frac{1}{2})$	$(2,\frac{1}{2})$	$(1,\frac{3}{2})$	$(0,-\frac{3}{2})$	$(-1,-\frac{1}{2})$	$(-2,\frac{1}{2})$	$(-3,\frac{3}{2})$
$3Dq-\zeta/2$	$\sqrt{2}\zeta/\sqrt{3}$	0	0	$\sqrt{15}Dq$	0	0
$\sqrt{2}\zeta/\sqrt{3}$	$-7Dq+\zeta/3$	$\sqrt{5}\zeta/\sqrt{6}$	0	0	$5Dq$	0
0	$\sqrt{5}\zeta/\sqrt{6}$	$Dq+\zeta/2$	0	0	0	$\sqrt{15}Dq$
0	0	0	$6Dq$	ζ	0	0
$\sqrt{15}Dq$	0	0	ζ	$Dq+\zeta/6$	$\sqrt{10}\zeta/3$	0
0	$5Dq$	0	0	$\sqrt{10}\zeta/3$	$-7Dq-\zeta/3$	$\zeta/\sqrt{2}$
0	0	$\sqrt{15}Dq$	0	0	$\zeta/\sqrt{2}$	$3Dq-3\zeta/2$

block 3: $\{(3,-1/2),(2,1/2),(1,3/2),(0,-3/2),$
$(-1,-1/2),(-2,1/2),(-3,3/2)\},$

and

block 4: $\{(3,-3/2),(2,-1/2),(1,1/2),(0,3/2),$
$(-1,-3/2),(-2,-1/2),(-3,1/2)\},$

Furthermore, because block 2 contains basis functions which are time reversed (i.e., the signs of the projections M_L and M_S are reversed) as compared to block 1, the Hamiltonian matrices for blocks 1 and 2 must be identical in the absence of an external magnetic field, as required by Kramers's theorem.[33] Likewise, block 4 contains the time-reversed basis functions as compared to those of block 3, and the Hamiltonian matrices for blocks 3 and 4 are also identical in the absence of an external magnetic field. As a result, the energies of all states deriving from the $3d^3,{}^4F$ term of Ti^+ may be obtained from the diagonalization of blocks 1 and 3.

The spin–orbit Hamiltonian is readily evaluated in terms of the atomic spin–orbit parameter, $\zeta_{3d}(Ti^+)$,[34] and the crystal field Hamiltonian may be expressed in terms of the ligand field parameter, Dq,[35] to give the Hamiltonian matrices for blocks 1 and 3 listed in Table II. These matrices have been checked to ensure that they give the known eigenvalues for the two cases $Dq=0$, $\zeta\neq 0$ (corresponding to a free, gas-phase $d^3,{}^4F$ ion) and $\zeta=0$, $Dq\neq 0$ (corresponding to a $d^3,{}^4F$ ion in an octahedral crystal field with no spin–orbit interaction). By smoothly varying the value of $Dq/(Dq+\zeta)$ from 0 to 1, one may correlate the energy levels of a $d^3,{}^4F$ ion from the limit of a free ion (characterized by the levels ${}^4F_J$, $J=3/2$, 5/2, 7/2, and 9/2) to the limit of an ion in a strong crystal field with vanishing spin–orbit interaction (characterized by the terms ${}^4A_{2g}$, ${}^4T_{2g}$, and ${}^4T_{1g}$). At intermediate values of $Dq/(Dq+\zeta)$ nine distinct energy levels emerge, and it becomes necessary to characterize the system using the $O_h^{(2)}$ double group notation. The character table for this double group is provided in Table III.[36] The resulting correlation diagram is displayed in Fig. 3, with the energy levels of the free ion labeled as ${}^4F_J$, the levels resulting in the limit $\zeta=0$, $Dq\neq 0$ labeled according to the O_h point group, and the levels in the intermediate range labeled according to the $O_h^{(2)}$ double group. To keep the energy levels on a convenient scale, the energy levels are divided by $6Dq+\zeta$ prior to plotting.

It is well-known that the energy levels deriving from a tetrahedral configuration may be obtained from the results for an octahedral configuration simply by replacing Dq with the value $-4Dq/9$.[33] For negative values of the abscissa, Fig. 3 also displays the results expected for a $d^3,{}^4F$ ion in a tetrahedral environment, generated by replacing Dq with $-4Dq/9$ in the Hamiltonian matrices of Table II and solving for the energy levels. It is useful to note that regardless of whether the site has T_d or O_h symmetry, the ground level remains fourfold degenerate throughout this correlation diagram. It is also easily shown that the energy levels deriving from the cuboctahedral arrangement of 12 ligands corresponding to site (i) may be obtained from the results for an octahedral configuration simply by replacing Dq with $-Dq/2$.[33] Thus a cuboctahedral substitutional site would be expected to provide a level structure and g value similar to that predicted for a tetrahedral interstitial site. Of course, in addition to energy levels, the matrix diagonalization procedure also provides wave functions as linear combinations of the basis set wave functions, and these are particularly useful when examining the magnetic properties of the resulting states.

C. Splitting of the fourfold degenerate ground level in a magnetic field

To compare the measured g values with those predicted by the above model, one must consider the Zeeman Hamiltonian which describes the interaction of the system with an externally applied magnetic field, $\mathbf{H}_0$. This is given by

TABLE III. Character table for the $O_h^{(2)}$ double group.[a]

$O_h^{(2)}$	E	R	$4C_3^2R$ $4C_3$	$4C_3^2$ $4C_3R$	$3C_2$ $3C_2R$	$3C_4^3R$ $3C_4$	$3C_4^3$ $3C_4R$	$6C_2'$ $6C_2'R$	i	Ri	$4C_3^2Ri$ $4C_3i$	$4c_3^2i$ $4C_3Ri$	$3C_2i$ $3C_2Ri$	$3C_4^3Ri$ $3C_4i$	$3C_4^3i$ $3C_4Ri$	$6C_2'i$ $6C_2'R$	
A_{1g}	1	1	1	1	1	1	1	1	1	1	1	1	1	1	1	1	$x^2+y^2+z^2$
A_{2g}	1	1	1	1	1	−1	−1	−1	1	1	1	1	1	−1	−1	−1	
E_g	2	2	−1	−1	2	0	0	0	2	2	−1	−1	2	0	0	0	
T_{1g}	3	3	0	0	−1	1	1	−1	3	3	0	0	−1	1	1	−1	(R_x,R_y,R_z)
T_{2g}	3	3	0	0	−1	−1	−1	1	3	3	0	0	−1	−1	−1	1	
$E_{1/2g}$	2	−2	1	−1	0	$\sqrt{2}$	$-\sqrt{2}$	0	2	−2	1	−1	0	$\sqrt{2}$	$-\sqrt{2}$	0	$S=1/2$
$E_{5/2g}$	2	−2	1	−1	0	$-\sqrt{2}$	$\sqrt{2}$	0	2	−2	1	−1	0	$-\sqrt{2}$	$\sqrt{2}$	0	
$G_{3/2g}$	4	−4	−1	1	0	0	0	0	4	−4	−1	1	0	0	0	0	$S=3/2$
A_{1u}	1	1	1	1	1	1	1	1	−1	−1	−1	−1	−1	−1	−1	−1	
A_{2u}	1	1	1	1	1	−1	−1	−1	−1	−1	−1	−1	−1	1	1	1	
E_u	2	2	−1	−1	2	0	0	0	−2	−2	1	1	−2	0	0	0	
T_{1u}	3	3	0	0	−1	1	1	−1	−3	−3	0	0	1	−1	−1	1	(x,y,z)
T_{2u}	3	3	0	0	−1	−1	−1	1	−3	−3	0	0	1	1	1	−1	
$E_{1/2u}$	2	−2	1	−1	0	$\sqrt{2}$	$-\sqrt{2}$	0	−2	2	−1	1	0	$-\sqrt{2}$	$\sqrt{2}$	0	
$E_{5/2u}$	2	−2	1	−1	0	$-\sqrt{2}$	$\sqrt{2}$	0	−2	2	−1	1	0	$\sqrt{2}$	$-\sqrt{2}$	0	
$G_{3/2u}$	4	−4	−1	1	0	0	0	0	−4	4	1	−1	0	0	0	0	

[a]Modified from Ref. 36.

$$\hat{H}^{\text{Zeeman}}=\beta_e H_0 \sum_i (\hat{l}_i+g_e\hat{\mathbf{s}}_i), \tag{4.1}$$

where i runs over all electrons in the system, l_i is the orbital angular momentum operator for electron i, $\hat{\mathbf{s}}_i$ is the spin angular momentum operator for electron i, β_e is the Bohr magneton, and $g_e=2.0023$.

Even at a magnetic field strength of 10 000 G, the Zeeman interaction only reaches a magnitude of a few cm^{-1}. This is at least a factor of 50 less than the expected separation between the $G_{3/2g}$ ground state of Ti^+ in an octahedral environment and the first excited state. It therefore makes sense to evaluate the effects of the magnetic field by treating $\hat{H}^{\text{Zeeman}}$ as a perturbation acting on the zeroth-order wave functions obtained from the crystal field plus spin–orbit analysis given above. To first order in perturbation theory it is then only necessary to evaluate the Hamiltonian matrix for $\hat{H}^{\text{Zeeman}}$ on a basis consisting of the four degenerate wave functions belonging to the $G_{3/2g}$ representation, which form the ground state of the octahedral $TiNe_6^+$ or $TiAr_6^+$ complex. Diagonalization of this 4×4 matrix then provides the splitting of the $G_{3/2g}$ states in a magnetic field.

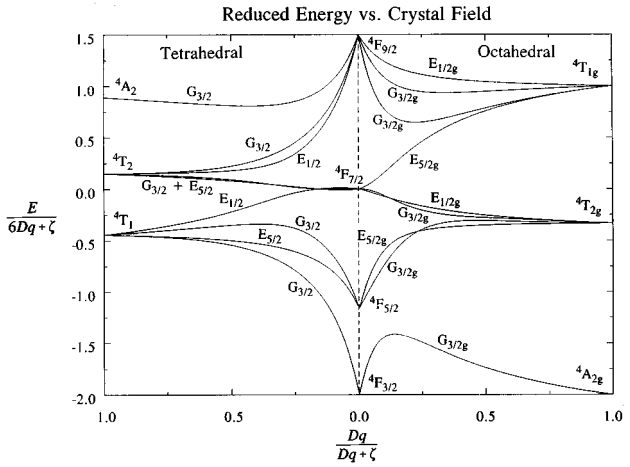

FIG. 3. Correlation diagram for a $d^3,{}^4F$ central ion in an octahedral or tetrahedral field, showing the splitting of the levels as functions of Dq and ζ. Energies are arbitrarily plotted in units of $6Dq+\zeta$ to keep the curves on a meaningful scale. The abscissa provides the value of $Dq/(Dq+\zeta)$, which ranges between 0 (a free gas-phase ion) and 1 (a system in which spin–orbit effects are negligible compared to the crystal field). The levels are labeled by the free-ion terms ^4F_J for $Dq/(Dq+\zeta)=0$, by the O_h point group labels for $Dq/(Dq+\zeta)=1$, and by the irreducible representations of the $O_h^{(2)}$ double group in the intermediate regime. The left-hand side of the diagram presents the analogous information for the tetrahedral coordination of a $d^3,{}^4F$ ion, with labels taken from the T_d and $T_d^{(2)}$ point groups.

According to convention, the states which are split from the $G_{3/2g}$ set of states are labeled according to a quantum number, M, which takes on the values $M=3/2$, $1/2$, $-1/2$, and $-3/2$, and the Zeeman contribution to the energy is taken as $\beta_e H_0 g M$, where g describes the strength of the Zeeman splitting. In the limiting case of a free atomic ion in a $^4F_{3/2}$ state ($Dq=0$), the values of M correspond to the allowed projections of the total angular momentum, J, on the z axis, and g reduces to the following formula for g_J,[37]

$$g_J=\frac{1}{2J(J+1)}[(g_e+1)J(J+1) -(g_e-1)(L(L+1)-S(S+1))]=0.3986$$
$$\text{for } L=3,\quad S=\frac{3}{2},\quad J=\frac{3}{2}. \tag{4.2}$$

Approximating $g_e\approx2$, this gives the more usual Landé expression for g_J:

$$g_J\approx1+\frac{J(J+1)+S(S+1)-L(L+1)}{2J(J+1)}=0.400$$
$$\text{for } L=3,\quad S=\frac{3}{2},\quad J=\frac{3}{2}. \tag{4.3}$$

Likewise, for the case of an ion in a strong crystal field with no spin–orbit interaction ($\zeta=0$), the values of M correspond to the allowed projections of the total electron spin, S, on the z axis, and g reduces to $g_e=2.0023$. In the intermediate regime, where both spin–orbit and crystal field interactions occur, the values of $M=3/2$, $1/2$, $-1/2$, and $-3/2$ are somewhat arbitrary, no longer corresponding to the z component of a well-defined angular momentum. Under this circumstance it is no longer necessary that the Zeeman energy follow the form of $E^{\text{Zeeman}}=\beta_e H_0 gM$, with M restricted to $\pm 3/2$, $\pm 1/2$.

To evaluate the Zeeman splitting of the ground state at any point in the correlation diagram of Fig. 3 we have calculated the matrix elements of $\hat{H}^{\text{Zeeman}}$ within the basis set obtained for the $G_{3/2g}$ set of states. This was done by writing each of these four states, ϕ_i ($i=1$–4), in terms of a superposition of the original basis functions listed in Table I, as

$$|\phi_i\rangle=\sum_{M_L,M_s} C^i_{M_L,M_S}|L,M_L\rangle|S,M_S\rangle, \tag{4.4}$$

leading to a diagonal Hamiltonian matrix with diagonal elements given by

$$H^{\text{Zeeman}}_{ii}=\beta_e H_0 \sum_{M_L,M_S} |C^i_{M_L,M_S}|^2(M_L+g_e M_S). \tag{4.5}$$

For the limiting case $Dq=0$ (corresponding to the free Ti^+ $3d^3,{}^4F$ ion) this approach led to Zeeman energies following the formula $E^{\text{Zeeman}}=\beta_e H_0 gM$, with g given by the Landé value of $g_J=0.3986$. Likewise, a calculation using $\zeta=0$ (corresponding to a ${}^4A_{2g}$ state uncontaminated by any spin–orbit mixing with the ${}^4T_{2g}$ and ${}^4T_{1g}$ states) gave the expected free-electron value of $g_e=2.0023$.

In the intermediate regime between $Dq/(Dq+\zeta)=0$ and 1 or for ions trapped in tetrahedral interstitial or cuboctahedral substitutional sites, the external magnetic field does indeed split the fourfold degeneracy of the $G_{3/2g}$ level, but the energy spacing between the resulting states is not equal, so it becomes impossible to use a single value of g in the formula $E^{\text{Zeeman}}=\beta_e H_0 gM$ (with $M=\pm 3/2$, $\pm 1/2$) to describe the behavior of the four energy levels. Instead, it is found that one value of g (designated by $g_{3/2}$) pertains to the more strongly affected levels (arbitrarily designated by $M=\pm 3/2$), while another value (designated by $g_{1/2}$) pertains to the less strongly affected levels (designated by $M=\pm 1/2$). The magnetic splitting of the levels as a function of $Dq/(Dq+\zeta)$ is depicted in Fig. 4, along with values of $g_{3/2}$ and $g_{1/2}$, again as functions of $Dq/(Dq+\zeta)$.

Figure 4 demonstrates that for free ions and for ions in octahedral sites with $Dq/(Dq+\zeta)>0.5$, this anomalous splitting pattern requiring distinct values for $g_{1/2}$ and $g_{3/2}$ will probably not be observed. Indeed, for $Dq/(Dq+\zeta)>0.5$ the reduction in either $g_{3/2}$ or $g_{1/2}$ from g_e follows the previously reported expression,[33–37]

$$g=g_e-\frac{8}{30}\frac{\zeta_{3d}}{Dq}. \tag{4.6}$$

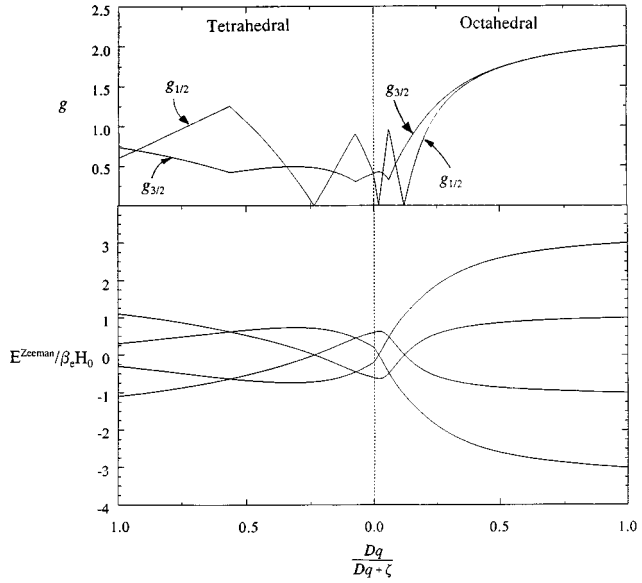

FIG. 4. Zeeman energy (lower panel) of the ground ($G_{3/2}$, ${}^4F_{3/2}$, $G_{3/2g}$, or ${}^4A_{2g}$) set of states (in units of $\beta_e H_0$) for values of $Dq/(Dq+\zeta)$ ranging from 0 to 1, in both the tetrahedral and octahedral ligand arrangements. The resulting g values for the more strongly affected ($g_{3/2}$) and less strongly affected ($g_{1/2}$) Zeeman levels are displayed in the upper panel.

to an accuracy within 0.6% in the final value of g, and $|g_{3/2}-g_{1/2}|<0.0052$.

To our knowledge no $d^3,{}^4F$ ion isolated in an octahedral site has ever been found to display the unusual, unsymmetrical Zeeman pattern predicted in Fig. 4 for small values of $Dq/(Dq+\zeta)$. Such effects would only be observed in systems with small crystal-field parameters, Dq, or large spin–orbit parameters, ζ. Given the strength of the Coulomb interaction between the central ion and the ligands, it seems doubtful that such effects would be observed in ionic systems except for ions trapped in tetrahedral interstitial or cuboctahedral substitutional sites. The absence of such strange effects in the ESR spectrum of Ti^+ in neon or argon may be taken as strong evidence for its isolation in the octahedral interstitial site, as opposed to the alternative sites (i) or (iii).

The observed values of g for Ti^+ isolated in neon and in argon (1.934 and 1.972) correspond to values of $Dq/(Dq+\zeta)$ of 0.7975 and 0.8983, respectively. From the energy levels of the gas phase $3d^3,{}^4F$ Ti^+ ion,[1] $\zeta_{3d}(Ti^+)$ may be derived to be 87.89 cm^{-1}, permitting Dq to be derived for the Ti^+ ion in neon and argon as 346 and 776 cm^{-1}, respectively. Note that for these parameters the difference between $g_{3/2}$ and $g_{1/2}$ is unobservably small (0.000 081 and 0.000 007 for neon and argon, respectively).

D. Physical interpretation of *Dq*

In the model of a central transition metal ion surrounded by ligands which may be represented as point charges, Dq is given by the expression[33,35]

$$Dq=\frac{1}{6}ze^2\frac{\langle r^4\rangle}{d^5}, \tag{4.7}$$

where the ligands consist of a set of point charges of magnitude $-ze$ located a distance d from the central ion, and $\langle r^4\rangle$ gives the expectation value of r^4 for the d orbitals of the central ion. For a Ti^+ ion isolated in a rare gas matrix, however, the ligands have no net charge and a different expression must be considered. If we treat the ligands as point dipoles of magnitude μ located a distance d from the central ion, Dq is given instead by[33]

$$Dq=\frac{5}{6}\,e\mu\,\frac{\langle r^4\rangle}{d^6}. \tag{4.8}$$

Finally, for the case of ligands which have no permanent dipole moment but which develop an induced dipole moment due to the charged central ion, μ is given by $\alpha e/r^2$, giving

$$Dq=\frac{5}{6}\,e^2\alpha\,\frac{\langle r^4\rangle}{d^8}. \tag{4.9}$$

It is well-known that none of these expressions work very well for typical octahedral transition metal complexes, primarily due to covalent interactions between the central ion and the ligands. In the case of a Ti^+ ion isolated in a neon or argon matrix, however, one might think that the inert nature of the rare gas would make Eq. (4.9) more applicable. Employing a value of $\langle r^4\rangle$ calculated by a numerical Hartree–Fock procedure for the $3d^3,{}^4F$ state of Ti^+ ($\langle r^4\rangle_{3d}=2.265$ Å^4)[38] and the accepted polarizabilities of neon and argon ($\alpha_{Ne}=0.3946$ Å^3; $\alpha_{Ar}=1.64$ Å^3),[39] along with the Ti^+–rare gas distances expected for the octahedral interstitial site ($d=2.231$ Å for neon, $d=2.656$ Å for argon), however, Eq. (4.9) predicts Dq values for neon and argon matrices of 141 and 145 cm^{-1}, respectively. These are substantially smaller than the Dq values found from an analysis of the measured g values ($Dq=346$ and 776 cm^{-1} for neon and argon, respectively).

One possibility which must be considered is that by limiting our consideration to the $3d^3,{}^4F$ term we have missed some of the essentials of the system. In particular, the $3d^3,{}^4P$ term is mixed with the $3d^3,{}^4F$ term by the crystal field Hamiltonian, causing what may be considered a ligand-induced configuration interaction between the ${}^4T_{1g}({}^4F)$ and ${}^4T_{1g}({}^4P)$ terms. Because spin–orbit interaction couples the ${}^4T_{1g}({}^4F)$ term to the ${}^4A_{2g}({}^4F)$ ground term and this is responsible for the departure of g from the free-electron value of 2.0023, any disturbance of the ${}^4T_{1g}({}^4F)$ term could conceivably affect the observed g value, discrediting the analysis presented above. To test this hypothesis we have expanded the basis set to include the states corresponding to the $3d^3,{}^4P$ term, have evaluated the matrix elements of both the crystal field and spin–orbit Hamiltonian, and have explicitly tested the resulting effect on g. Although a definite effect on g occurs for small values of $Dq/(Dq+\zeta)$, the $3d^3,{}^4P$ term of Ti^+ lies too high in energy to significantly alter the final derived values of Dq for neon or argon.

Two probable causes exist for this discrepancy between the values of Dq derived from the ESR measurements and those predicted by treating the rare gas atoms as having an induced point dipole moment. First, it is simply incorrect to consider a rare gas atom less than 3 Å from a Ti^+ ion as a point dipole. There will be a significant charge separation in the rare gas atom, such that the center of the negative charge is substantially closer to the Ti^+ ion than is the center of the positive charge. A more realistic model might overcome this difficulty by treating the dipole induced in the rare gas atom as a dipole of finite dimension, rather than as a point dipole. This would lead to an increase in the predicted value of Dq, since the negative charge on the argon would now be substantially closer to the Ti^+ ion. This effect would then bring the expected value of Dq more into line with that derived from experiment. A second problem in the treatment is the assumption that the insertion of a Ti^+ ion into an octahedral interstitial site will leave the soft rare gas lattice unperturbed. Clearly the strong ion-induced dipole force will cause a local distortion of the rare gas lattice, possibly pulling the rare gas atoms closer to the central Ti^+ ion and increasing the value of Dq. Unfortunately, it is difficult to accurately model the magnitude of these two effects, making further progress along these lines problematic at best. Regardless of the physical interpretation of Dq, however, all of the ESR observations are in accord with the Ti^+ ion occupying an octahedral site in the rare gas lattice, and meaningful values of Dq are obtained from the analysis. It would be of considerable interest to compare these Dq values to *ab initio* quantum chemical calculations on a $Ti^+(Rg)_6$ ion in vacuum.

The observed ESR characteristics also strongly resemble those of the well-known isoelectronic Cr^{+3} ($3d^3$) radical ion located in an octahedral site in magnesium oxide.[40] This well-established example of a $3d^3,{}^4A_{2g}$ radical ion supports our arguments for a similar ground state assignment for Ti^+ ($3d^3$) in neon and argon matrices. The Cr^{+3} line shape is highly isotropic and its magnetic parameters are $g=1.9796$ and $A(^{53}Cr)=49$ MHz. The calculated atomic A_{iso} parameters for the $4s$ electron in neutral ^{53}Cr and ^{47}Ti are fortuitously similar at -748 and -782 MHz, respectively.[41] (Both have negative magnetic moments.) By comparison, the small A values observed for $^{47}Ti^+$ (64 MHz in neon) and Cr^{+3} (49 MHz in MgO) are consistent with the lack of direct $4s$ admixture in the assumed $3d^3$ electronic configuration for these two isoelectronic metal ions.

V. CONCLUSION

An ESR study of laser-ablated titanium isolated in neon and argon matrices displays a spectrum with a large matrix-dependent g shift, which is assigned to a matrix isolated $3d^3,{}^4F$ Ti^+ ion in an octahedral environment. This is supported by the narrow, symmetric line in the ESR spectrum and by the small hyperfine structure observed. A crystal-field study of the behavior of a $d^3,{}^4F$ ion isolated in a tetrahedral, octahedral, or cuboctahedral environment supports the assignment to an octahedral $Ti^+(Rg)_6$ species, and using the atomic spin–orbit parameter, ζ permits the Dq value to be derived. Although the resulting values of Dq for both Ne and Ar are inconsistent with a model in which the rare gas is a polarizable point species and the rare gas lattice is unperturbed by the presence of an interstitial Ti^+ ion, it is argued

that these assumptions are unrealistic and that the measured g value does provide a reasonable estimate of Dq. Finally, it is also noted that for small values of $Dq/(Dq+\zeta)$, or for a d^3,^4F ion in a tetrahedral environment an as yet unobserved, unequal Zeeman splitting of the fourfold degeneracy is expected. This is predicted to cause a departure of the Zeeman energies from $E^{\text{Zeeman}}=\beta_e H_0 g M$, with $M=\pm 3/2, \pm 1/2$. For these situations it becomes necessary to define two values of g, corresponding to the more strongly $(g_{3/2})$ and less strongly $(g_{1/2})$ effected Zeeman levels, respectively. It would be of great interest to find experimental verification of this prediction.

ACKNOWLEDGMENTS

Project grant support from the National Science Foundation Grant No. (CHE-9319291) and an NSF-REU site grant to Furman University is gratefully acknowledged. Equipment and student support was made available from a Duke Endowment Grant to Furman University, the 3 M Company, and a DuPont College Science Grant. M.D.M. thanks the U.S. Department of Energy Contract No. (DE-FG03-93ER143368) for support of research on unsaturated transition metal–ligand complexes. M.D.M. also acknowledges the donors of the Petroleum Research Fund, administered by the American Chemical Society, for partial support of this research.

[1] C. Corliss and J. Sugar, J. Phys. Chem. Ref. Data **8**, 1 (1979).
[2] Unpublished ESR spectra attributed to Fe^+ (^6D) and Ru^+(^4F) have been observed by R. J. Van Zee and W. Weltner, Jr. in rare gas matrices. Pulsed laser vaporization was the generation method employed. Matrix trapping using conventional high temperature vaporization (where ions would not likely be produced) did not produce the ESR spectra (private communication).
[3] H. Partridge and C. W. Bauschlicher, Jr., J. Phys. Chem. **98**, 2301 (1994).
[4] D. Lessen and P. J. Brucat, Chem. Phys. Lett. **149**, 10 (1988).
[5] K. Jacobi, D. Scheisser, and D. K. Kolb, Chem. Phys. Lett. **69**, 113 (1980); R. Grinter and D. R. Stern, J. Chem. Soc. Faraday Trans. 2 **79**, 1011 (1983); B. Breithaupt, J. E. Hulse, D. M. Kolb, H. H. Rotermund, W. Schroeder, and W. Schrittenlacher, Chem. Phys. Lett. **95**, 513 (1983).
[6] W. Weltner, Jr., *Magnetic Atoms and Molecules* (Dover, Mineola, NY, 1989).
[7] J. H. Ammeter and D. C. Schlosnagle, J. Chem. Phys. **59**, 4784 (1973).
[8] A. J. Merer, Annu. Rev. Phys. Chem. **40**, 407 (1989).
[9] J. M. Dyke, B. W. J. Gravenor, G. D. Josland, R. A. Lewis, and A. Morris, Mol. Phys. **53**, 465 (1984); A. D. Sappey, G. Eiden, J. E. Harrington, and J. C. Weisshaar, J. Chem. Phys. **90**, 1415 (1989).
[10] L. B. Knight, Jr., Acc. Chem. Res. **19**, 313 (1986).
[11] L. B. Knight, Jr., *Chemistry and Physics of Matrix-Isolated Species*, edited by L. Andrews and M. Moskovits (North Holland, Amsterdam, 1989), Chap. 7.
[12] L. B. Knight, Jr., *Radical Ionic Systems*, edited by A. Lund and M. Shiotani (Kluwer Academic, Dordrecht, 1991), pp. 73–97.
[13] Rare Gas Matrix Isolation Spectroscopy, edited by P. H. Kasai (Review) (to be published).
[14] R. J. Van Zee and W. Weltner, Jr., High Temp. Sci. **17**, 181 (1984).
[15] R. J. Van Zee and W. Weltner, Jr., Chem. Phys. Lett. **107**, 173 (1984).
[16] R. J. Van Zee, S. Li, and W. Weltner, Jr., J. Chem. Phys. **103**, 2762 (1995).
[17] G. V. Chertihin and L. Andrews, J. Phys. Chem. **98**, 5891 (1994).
[18] L. B. Knight, Jr., J. O. Herlong, R. Babb, E. Earl, D. W. Hill, and C. A. Arrington, J. Phys. Chem. **95**, 2732 (1991).
[19] L. B. Knight, Jr., K. Kerr, M. Villanueva, A. J. McKinley, and D. Feller, J. Chem. Phys. **97**, 5363 (1992).
[20] L. B. Knight, Jr., G. C. Jones, G. M. King, R. M. Babb, and A. J. McKinley, J. Chem. Phys. **103**, 497 (1995).
[21] A. J. McKinley and J. Michl, J. Phys. Chem. **95**, 2674 (1991).
[22] L. B. Knight, Jr., A. J. McKinley, R. M. Babb, D. W. Hill, and M. D. Morse, J. Chem. Phys. **99**, 7376 (1993).
[23] Unpublished measurements in the Furman ESR laboratory have shown that the g value of the methyl radical in neon and argon equals 2.0020(2).
[24] L. B. Knight, Jr., S. T. Cobranchi, and E. Earl, J. Chem. Phys. **88**, 7348 (1988).
[25] B. S. Ault and L. Andrews, J. Chem. Phys. **63**, 1411 (1975); V. E. Bondybey and J. H. English, *ibid*. **71**, 777 (1979).
[26] D. G. Henshaw, Phys. Rev. **111**, 1470 (1958).
[27] G. L. Pollack, Rev. Mod. Phys. **36**, 748 (1964).
[28] J. Bushnell, P. Maitre, P. R. Kemper, and M. T. Bowers, J. Phys. Chem. (to be published).
[29] P. A. M. Van Koppen, J. Bushnell, P. R. Kemper, J. Perry, and M. T. Bowers, J. Am. Chem. Soc. (to be published).
[30] J. E. Bushnell, P. R. Kemper, and M. T. Bowers, J. Phys. Chem. **99**, 15602 (1995).
[31] J. E. Bushnell, P. R. Kemper, P. Maitre, and M. T. Bowers, J. Am. Chem. Soc. **116**, 9710 (1994).
[32] P. Weis, P. R. Kemper, and M. T. Bowers (unpublished).
[33] J. S. Griffith, *The Theory of Transition Metal Ions* (Cambridge University Press, Cambridge, 1961).
[34] H. Lefebvre-Brion and R. W. Field, *Perturbations in the Spectra of Diatomic Molecules* (Academic, Orlando, 1986).
[35] B. N. Figgis, *Introduction to Ligand Fields* (Interscience, New York, 1966).
[36] A. Abragam and B. Bleany, *Electron Paramagnetic Resonance of Transition Ions* (Dover, New York, 1986).
[37] C. Froese-Fischer, *The Hartree–Fock Method for Atoms. A Numerical Approach* (Wiley, New York, 1977).
[38] T. M. Miller and B. Bederson, Adv. At. Mol. Phys. **13**, 1 (1977).
[39] J. E. Wertz and J. R. Bolton, *Electron Spin Resonance* (Chapman and Hall, London, 1986).
[40] J. R. Morton and K. F. Preston, J. Magn. Reson. **30**, 577 (1978).